

Atomic layer deposition for electrochemical energy generation and storage systems

Qing Peng, Jay S. Lewis, Paul G. Hoertz, Jeffrey T. Glass, and Gregory N. Parsons

Citation: *Journal of Vacuum Science & Technology A* **30**, 010803 (2012); doi: 10.1116/1.3672027

View online: <http://dx.doi.org/10.1116/1.3672027>

View Table of Contents: <http://scitation.aip.org/content/avs/journal/jvsta/30/1?ver=pdfcov>

Published by the AVS: Science & Technology of Materials, Interfaces, and Processing

Articles you may be interested in

[Emission constrained economic dispatch for hybrid energy system in the presence of distributed generation and energy storage](#)

J. Renewable Sustainable Energy **7**, 013125 (2015); 10.1063/1.4906930

[Atomic layer deposition for nanostructured Li-ion batteries](#)

J. Vac. Sci. Technol. A **30**, 010801 (2012); 10.1116/1.3660699

[Study of amorphous lithium silicate thin films grown by atomic layer deposition](#)


J. Vac. Sci. Technol. A **30**, 01A106 (2012); 10.1116/1.3643349

[Power System Concepts for the Lunar Outpost: A Review of the Power Generation, Energy Storage, Power Management and Distribution \(PMAD\) System Requirements and Potential Technologies for Development of the Lunar Outpost](#)





AIP Conf. Proc. **813**, 1083 (2006); 10.1063/1.2169289

[Lithium storage in polymerized carbon nitride nanobells](#)

Appl. Phys. Lett. **79**, 3500 (2001); 10.1063/1.1419034



Instruments for Advanced Science

<p>Contact Hiden Analytical for further details: W www.HidenAnalytical.com E info@hiden.co.uk</p> <p>CLICK TO VIEW our product catalogue</p>	 <p>Gas Analysis</p> <ul style="list-style-type: none"> » dynamic measurement of reaction gas streams » catalysis and thermal analysis » molecular beam studies » dissolved species probes » fermentation, environmental and ecological studies 	 <p>Surface Science</p> <ul style="list-style-type: none"> » UHV TPD » SIMS » end point detection in ion beam etch » elemental imaging - surface mapping 	 <p>Plasma Diagnostics</p> <ul style="list-style-type: none"> » plasma source characterization » etch and deposition process reaction » kinetic studies » analysis of neutral and radical species 	 <p>Vacuum Analysis</p> <ul style="list-style-type: none"> » partial pressure measurement and control of process gases » reactive sputter process control » vacuum diagnostics » vacuum coating process monitoring
---	--	--	--	--

Atomic layer deposition for electrochemical energy generation and storage systems

Qing Peng^{a)}

Electrical and Computer Engineering Department, Duke University, Durham, North Carolina 27708

Jay S. Lewis and Paul G. Hoertz

Research Triangle Institute, Research Triangle Park, North Carolina 27709

Jeffrey T. Glass^{b)}

Electrical and Computer Engineering Department, Duke University, Durham, North Carolina 27708

Gregory N. Parsons^{c)}

Department of Chemical and Biomolecular Engineering, North Carolina State University, 911 Partners Way, Raleigh, North Carolina 27695 and Research Triangle Institute, Research Triangle Park, North Carolina 27709

(Received 18 September 2011; accepted 1 December 2011; published 27 December 2011)

Clean renewable energy sources (e.g., solar, wind, and hydro) offers the most promising solution to energy and environmental sustainability. On the other hand, owing to the spatial and temporal variations of renewable energy sources, and transportation and mobility needs, high density energy storage and efficient energy distribution to points of use is also critical. Moreover, it is challenging to scale up those processes in a cost-effective way. Electrochemical processes, including photoelectrochemical devices, batteries, fuel cells, super capacitors, and others, have shown promise for addressing many of the abovementioned challenges. Materials with designer properties, especially the interfacial properties, play critical role for the performance of those devices. Atomic layer deposition is capable of precise engineering material properties on atomic scale. In this review, we focus on the current state of knowledge of the applications, perspective and challenges of atomic layer deposition process on the electrochemical energy generation and storage devices and processes. © 2012 American Vacuum Society. [DOI: 10.1116/1.3672027]

I. INTRODUCTION

A. Background

In order to alleviate the impact of greenhouse-gases on the global environment, it is predicted that by the year of 2050, at least 10 TW (10×10^{12} W) of power needs to be produced from carbon-neutral energy sources.¹ This is almost equal to the energy provided by all of today's energy sources combined. Several environmentally clean alternative renewable energy sources (e.g., wind, hydro, solar), are the most promising solutions to address this tremendous challenge.¹ For example, as an inexhaustible natural energy source, approximately 4.3×10^{20} J of energy strikes the earth every hour, which is roughly equal to the amount of energy needed for the entire human population over an entire year (4.5×10^{20} J).¹

Unfortunately, major challenges also exist beyond supplying such a large amount of energy from carbon-neutral sources. Owing to the transportation and mobility needs,² and temporal and spatial variation of renewable energy sources,¹ high density energy storage,³ and efficient energy distribution to points of use are critical issues as well. Cost effectively

scale-up energy production, distribution and storage systems presents another great challenge for energy sustainability.¹ Electrochemical processes offer promising solutions to these challenges, including photoelectrochemical (PEC) devices,^{1,4} batteries,^{2,3} fuel cells,⁵ super capacitors, and others.

B. Electrochemical processes

In a typical electrochemical process, the properties of the electrodes and electrolytes as well as the interfacial properties between the electrodes and electrolytes all play critical roles for the device performance.⁶ In order to achieve desired device performance including for example a high capacitance, high reliability and high energy conversion efficiency, one must utilize "designer materials" with tunable physical and chemical properties. This requires sophisticated methods to assemble materials at various scales, including molecular, nano, microscopic, and macroscopic levels. For this purpose, researchers develop and explore a variety of materials engineering methods. Each has their own advantages and disadvantages. In this review, we will mainly focus on the atomic layer deposition (ALD) process. Although ALD has been widely applied to microelectronics and other related applications over the past several decades,⁷ it is a relatively new

^{a)}Electronic mail: qing.peng@duke.edu

^{b)}Electronic mail: jeff.glass@duke.edu

^{c)}Electronic mail: gnp@ncsu.edu

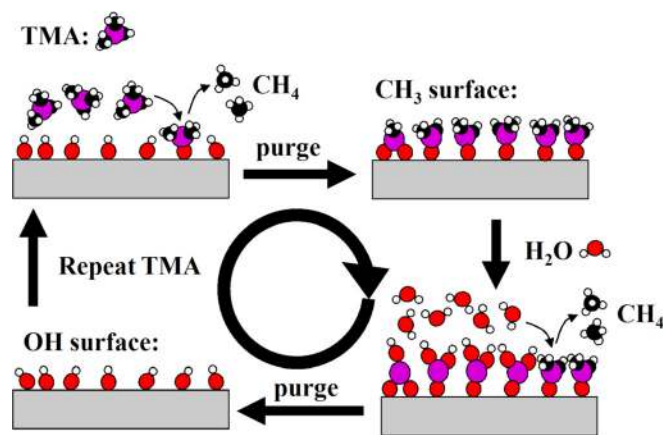


FIG. 1. (Color online) Simplified scheme of atomic layer deposition by using Al_2O_3 ALD as the example. TMA: Trimethyl aluminum. Reprinted with permission from Ref. 132 (copyright 2007 American Chemical Society).

technique that is just beginning to emerge as an important method for electrochemical devices and processes.

C. The unique nature of ALD processes

As shown in Fig. 1, ALD is a cyclic process involving sequential self-limiting surface reactions.^{7–10} During ALD, a volatile precursor (typically a metal-organic molecule) and a coreactant (typically oxidizing or reducing agent) are delivered in a time-sequence, isolated from each other by an inert gas purging step. This sequential delivery scheme eliminates homogeneous reactions, and permits the individual half-reactions to proceed to completion during each delivery cycle.^{7–10} Owing to the self-limiting nature, the coating thickness can be tuned to submonolayer precision over very large surface areas.^{7–10} Even more interesting is that by alternating different ALD chemistries, one can synthesize nanocomposites or even molecular composites with controlled compositions and properties.^{7–10} For most ALD processes, the reactants are introduced as vapor into a vacuum (1–2 Torr) reactor. The high diffusion coefficients of vapors and lack of surface tension, in conjunction with the cyclic surface reaction mechanism, enable highly conformal coverage onto substrates with high surface areas and complex morphologies. Due to these unique properties, ALD has attracted substantial interest in both the scientific and industrial communities for its potential to address a variety of challenges in energy related electrochemical processes.

II. ATOMIC LAYER DEPOSITION FOR PHOTOELECTROCHEMICAL WATER SPLITTING

A. Introduction to photoelectrochemical water splitting

Solar radiation is an attractive primary energy source. Conversion of solar energy into chemical fuel in a cost-effective way is considered to be a “holy grail”¹¹ of renewable energy. PEC processes offer the most promising ways to convert solar energy into fuel (e.g., H_2 , CH_3OH), especially H_2 .^{4,11,12} Since 1972,¹³ there has been substantial progress in PEC water split-

ting research to generate H_2 , particularly in understanding the mechanism and optimizing material performance.^{4,12,14–18} Principle diagrams of representative PEC water splitting devices, are shown in Fig. 2. The photoelectrode absorbs light, which excites valence electrons into the conduction band, leaving holes in the valence band. The excited electron/hole pair must then be separated and migrate to the interface between the semiconductor and electrolytes to react with the oxidizing agent (i.e., water/hydroxide) and reducing agent (i.e., water/protons) in the electrolyte respectively. Generally, for p-type semiconductor/liquid junction, electron migrates to the interface of junction and for n-type semiconductor/liquid junction, hole migrates to the interface junction.

In order to carry out the water splitting reaction efficiently, there are several important parameters that must be optimized.^{4,11,12,15}

- (1) The semiconductor conduction band edge must be more negative than the redox potential of H^+/H_2 (0 V versus NHE, while the valence band edge must be more positive than the redox potential of $\text{H}_2\text{O}/\text{O}_2$ (1.23 V versus NHE, as shown in Fig. 2(a)).^{11–13} This requirement can be relaxed by using a tandem cell [two semiconductors of small band gap connected in series, e.g., dual band gap device, as represented by Fig. 2(b)].^{11,12}
- (2) In order to maximize the amount of solar spectrum that is utilized, the band gap of the semiconductor should be ~ 2.0 eV since $\sim 46\%$ of natural sun light energy is from visible light and only 4% is from UV light.¹⁵ For instance, although the conduction band and valence band edges of TiO_2 straddle the redox potentials of H^+/H_2 and $\text{H}_2\text{O}/\text{O}_2$, the overall efficiency of water splitting reaction is less than 1%. It is primarily due to the large bandgap of TiO_2 (~ 3.0 eV), which allows only UV light to be absorbed to generate the excited electron-hole pairs. An alternative approach is to use a tandem cell to provide complementary light absorption for higher conversion efficiency as represented by Fig. 2(b).^{11,12} Dye sensitized electrode in PEC cells, as illustrated in Fig. 2(c),^{17,19,20} can also help absorb a broader spectrum of sunlight.
- (3) The photon-to-electron efficiency (quantum efficiency) of the PEC system needs to be high (close to 1), which requires a slow charge recombination rates, long charge separation lifetimes, and high mobilities of charge carriers. Smaller lengths for charge diffusion/transport, low densities of recombination centers, and competitive charge transfer rate relative to the recombination rate, promote higher quantum yields of charge separation and fuel production.
- (4) The overpotential, which is the additional voltage beyond the thermodynamic potential that is required to achieve a certain rate of the desired reaction, should be minimized. Many factors contribute to the overpotential, including the catalyst structure, the mechanism of water oxidation or reduction that is at play, the nature of the semiconductor/electrolyte surface, and the interplay between the surface and catalyst active sites.

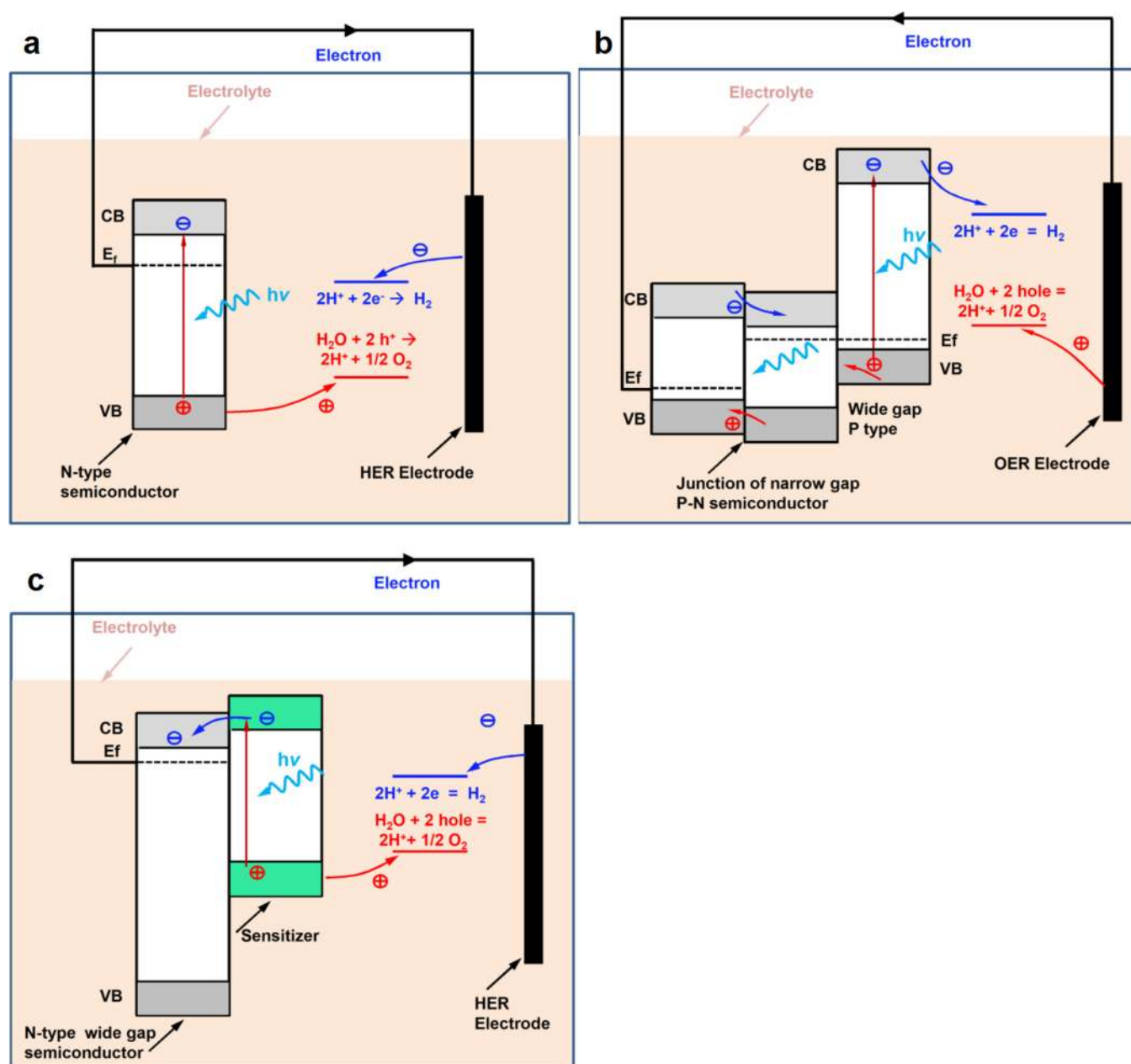


Fig. 2. (Color online) Principle diagram of water splitting process by using (a) single semiconductor/liquid junction; (b) photovoltaic cell assisted semiconductor/liquid junction; (c) dye sensitized semiconductor/liquid junction. CB: conduction band; VB: valence band; Ef: Fermi level; HER: hydrogen evolution reaction; OER: oxygen evolution reaction. For effective water splitting, electrons and holes need to have enough energy for HER and OER reaction. Electrodes need to be stable under dark and light condition. Detail mechanisms of different types of PEC cells have been discussed in other reviews Refs. 4, 11, 12.

(5) The semiconductor, catalyst and other components that compose the electrode need to be stable during the PEC process and in the dark. For example, Si (bandgap ~ 1.1 eV, absorbing a large part of sun spectrum), a potential photoanode candidate for water splitting, is chemically unstable at the water oxidation potential.²¹

Based on the above understanding, a wide range of material systems have been explored and different strategies for engineering materials to satisfy those requirements have been developed and reviewed in the literature.^{4,12,15,22,23} The PEC water splitting devices are classified into different types including single semiconductor/liquid junction cells,

multijunction tandem cells, dye sensitized semiconductor cell etc as shown by the examples in Fig. 2.^{11,12} Table I provides a list of some of the highest reported PEC water splitting efficiencies using either single photoelectrode or tandem cell arrangements. A few of the reports also present results regarding device performance under prolonged irradiation, and stability data for those devices is also included in the table. For single semiconductor/liquid junctions, the highest solar to hydrogen conversion efficiency to date is $\sim 13.3\%$ using a device fabricated with p-type indium phosphide, p-InP, decorated with Rh and Re catalysts.²⁴ However, the electrode surface's passivating oxide layer had to be restored every 5 min in order to maintain high efficiency

TABLE I. High performance photoelectrochemical water splitting device and associated device stability results.

Reference	Device architecture	Surface catalysts	Materials systems	Efficiency ^a (%)	Lifetime testing
Heller <i>et al.</i> (Ref. 24)	Photo-cathode	Ru, Re, or Rh @ cathode	p-InP	11.4–13.3	Requires periodic cycling to V_{oc} to maintain high efficiency
Turner <i>et al.</i> (Ref. 136)	Tandem PV	Pt @ cathode Pt @ anode	p-n GaInP ₂ /p-n GaAs	16.5	Not reported
Turner <i>et al.</i> (Ref. 25)	Tandem photo-cathode/PV ^b	Pt @ cathode Pt @ anode	p-GaInP ₂ /p-n GaAs	12.4	Photocurrent decrease from 120 to 105 mA/cm ² over 20 h
Licht <i>et al.</i> (Ref. 26)	Tandem PV	Pt @ cathode RuO ₂ @ anode	AlGaAs/Si	18.3	Stable photocurrent over 14 h
Bockris <i>et al.</i> (Ref. 27)	Tandem p/n-photo-electro-chemical	Pt @ cathode MnO ₂ /Pt @ anode	p-InP/n-GaAs	8.2	10% efficiency decrease during first hour, then remains constant for 10 h
Gratzel <i>et al.</i> (Ref. 4)	Tandem photo-anode/PV	Pt @ cathode	WO ₃ /DSSC PV	4.5	Not reported
Gratzel <i>et al.</i> (Refs. 12, 28)	Tandem photo-anode/PV	Pt @ cathode	Fe ₂ O ₃ /DSSC PV	2.2	Not reported

^aReported overall efficiency.

^bPV = photovoltaic cell

PEC working conditions. Single junction devices suffer either from electrode corrosion (small bandgap materials) or low absorption of visible light (large bandgap materials).^{4,12} Dual bandgap tandem cells, which can utilize more solar spectrum, can provide even higher efficiencies,^{4,12} and water splitting cells with high photon-to-fuel efficiencies have been reported. For example, Khaselev and Turner reported a conversion efficiency of 12.4% for the dual band structure device comprising a p-GaInP₂/Pt photocathode coupled with a p-n GaAs junction,²⁵ whose principle is shown in Fig. 2(b). The electrode was stable for more than 20 h before degradation. Licht *et al.* reported a complex AlGaAs/Si photovoltaic backed RuO₂/Pt electrode with a solar to hydrogen efficiency of ~18%.²⁶ The operational stability of the electrode was more than 12 h.²⁶ However, the cost for such a cell is prohibitive for large scale implementation due to the low production rate of high quality III-V semiconductors and precious metal catalysts. Bockris and coworkers constructed a 8.2% solar fuel cell consisting of a p-type single crystalline InP photocathode coated with Pt islands and an n-type single crystalline GaAs photoanode coated with a thin MnO₂ layer.²⁷ The efficiency of this device is quite impressive; however, the use of single crystal materials and materials with low earth abundance suggests expensive scale-up. Although progress has been made in PEC water splitting research and results are promising, significant development is needed to achieve a low-cost, high efficiency PEC water splitting device that also exhibits long-term stability preferably on the timescale of years.

Gratzel and coworkers have coupled low-cost dye-sensitized solar cell (DSSC) photovoltaic devices (see Sec. III for a more detailed description) with nanostructured n-type earth abundant photoanode materials such as Fe₂O₃ (Refs. 12, 28) and WO₃.⁴ The efficiencies of these devices are low

compared to the single-crystalline tandem cells mentioned above, but results suggest that low-cost and high efficiency water splitting devices could ultimately be achievable.

The discussion below presents what ALD can offer to address these research challenges and make PEC energy conversion more realistic.

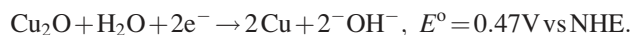
B. Atomic layer deposition for protecting photoelectrodes

To be commercially viable, photoelectrodes must be stable over long time periods,^{4,12,15,29,30} ideally for several years. The stability problem is exceptionally challenging owing to (1) the corrosive environment of the basic and acidic electrolytes in the dark or under illumination, (2) photocorrosion due to the presence of photodecomposition pathways that are promoted by the presence highly energetic holes and electrons under illumination; (3) corrosion caused by the products generated during electrochemical water oxidation and reduction. An important determinant of the photochemical stability of an electrode material is the electrochemical potential of the corrosion reaction (e.g., oxidation, metal cation reduction) and where it lays on an electrochemical scale with respect to water oxidation/reduction potentials. For water reduction at a photocathode, the electrochemical potential of the corrosion reactions should lie more negative than the H⁺/H₂ potential. For water oxidation at a photoanode, the corrosion reaction should ideally lie more positive than the H₂O/O₂ potential. Otherwise, corrosion will be thermodynamically favored over the desired water splitting half reactions.¹² For most elemental and nonoxide semiconductors, the electrode oxidation proceeds at a potential negative than the water oxidation, resulting in significant corrosion.³¹ In addition, highly energetic carriers available under illumination can promote reactions that would not readily proceed in the dark, although

it is important to note that some key corrosion reactions proceed readily in the dark. A common example is dark oxidation of p-type electrodes, such as Si, GaAs, GaP.³¹ For semiconductors with large bandgaps (e.g., TiO₂, Nb₂O₅), corrosion is less of an issue,⁴ however, the band gap limits the amount of visible light that can be absorbed. On the other hand, small bandgap materials which have good visible light absorption, are typically more prone to the undesirable (photo) corrosion side reactions.^{12,15,29,30}

Two approaches to achieve stable PEC device performance include (i) kinetically promoting the desired redox reaction (e.g., with a tuned catalyst or tuned redox couple) so that it becomes favored over the undesired corrosion reaction³² and (ii) blocking the undesired reaction by passivating the surface to oxidation or reduction, using organic³³ or inorganic passivation layers.^{29,30,34} Unfortunately, there are trade-offs in these two approaches. That is, catalysts that enhance the redox reaction rate also often promote the corrosion rate (catalyst with high selectivity desired) and surface passivation approaches typically impede the desired redox reaction rate. In the following section, the application of ALD for protecting electrodes from corrosion will be discussed.

As discussed in Sec. I, ALD offers a unique capability to coat complex geometries with a conformal and uniform film with well-controlled thickness down to the submonolayer level. Thimsen, Gratzel, and coworkers³⁵ have recently demonstrated nanolaminates formed by ALD for protecting Cu₂O (p-type oxide, bandgap ~ 2 eV) under solar illumination in the proton reduction (H₂ generation) environment. It is well-known that an unprotected Cu₂O photocathode is readily degraded to Cu under illumination at applied potential due to the following photodegradation reaction:



Several nanolaminate structures consisting of ZnO/Al₂O₃/TiO₂ layers, generated by ALD, were applied to Cu₂O and systematically evaluated.³⁵ The first interesting finding was that although TiO₂ satisfied the bandgap energetics requirement for acting as a protective layer, a TiO₂ ALD coating alone, even up to 30 nm, did not protect the Cu₂O electrode from undergoing photoreduction. This result was ascribed to pin holes in the TiO₂ ALD film. Secondly, a 20 nm ZnO ALD buffer layer between the Cu₂O and the 10 nm TiO₂ coating was found to help chemically stabilize the Cu₂O electrode, producing reasonably stable performance for about 1 h. The ZnO ALD process was believed to generate denser nucleation sites on the Cu₂O substrate and enhance the quality (i.e., reducing the number of pin holes), of the subsequent TiO₂ film grown by ALD. It is worth noting that the electrodeposited Cu₂O electrodes have a rough and irregular surface morphology as shown in Fig. 3(a). It is very challenging for other methods, including chemical vapor deposition, physical vapor deposition and sol-gel methods to form such a thin (~ 10 nm level) conformal protecting layer onto this type of surface. Thus, ALD offers a very attractive, if not the only viable

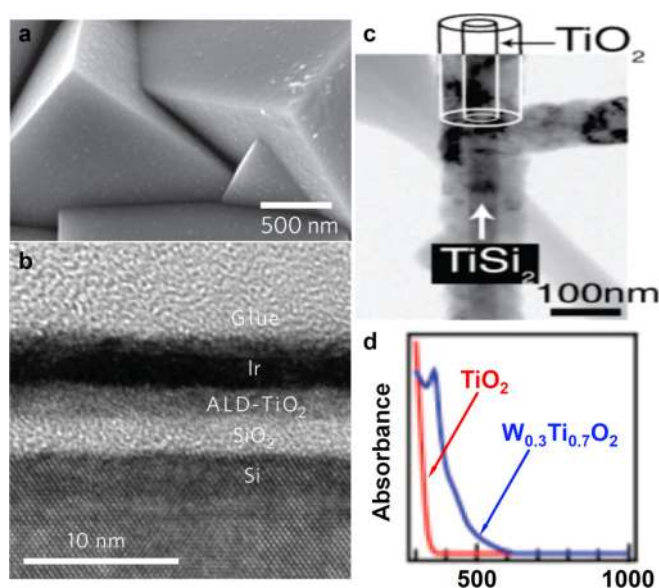


Fig. 3. (Color online) (a) SEM image of the Cu₂O electrodes after coated with 5 × (4 nm ZnO/0.17 nm Al₂O₃)/11 nm TiO₂ followed by electrodeposition of Pt nanoparticles. Reprinted with permission from Ref. 35 (copyright 2011 Nature Publication Group). (b) TEM image of the nanocomposite anode of Si/SiO₂/ALD TiO₂/Ir. Reprinted with permission from Ref. 37 (copyright 2011 Nature Publication Group). (c) TEM image of the core-shell TiSi₂/TiO₂ structure. Reprinted with permission from Ref. 39 (copyright 2009 American Chemical Society). (d) UV-vis spectra of ALD TiO₂ and ALD W doped TiO₂ (W_{0.3}Ti_{0.7}O₂). Reprinted with permission from Ref. 39 (copyright 2009 American Chemical Society).

method, to form a protective overcoat onto the substrate. The results also suggest that the protective properties of the ALD coating are further enhanced by doping the ZnO with Al₂O₃, which enhanced the conductivity of the ZnO and maintained the desired bandgap energetics.³⁵ This could potentially be further refined through prudent choice of dopant and doping levels to tune the band edge as desired.

The effect of ALD coatings on a nanostructured Fe₂O₃ photoelectrode was also evaluated by Gratzel *et al.*³⁶ An ultra-thin coating of Al₂O₃ (< 2 nm) resulted in a large overpotential drop by as much as 100 mV and significant increases in the photocurrent (from 0.24 to 0.85 mA/cm²) at 1.0 V versus the reversible hydrogen electrode under standard illumination conditions. The dramatic improvement in performance was ascribed to the passivation of surface states by the Al₂O₃ ALD process. It is interesting to note that a TiO₂ ALD overcoating onto the Fe₂O₃ photoelectrode did not show any improvement in the electrode performance. It would be valuable to elucidate the mechanism behind of the different effects of TiO₂ and Al₂O₃ overcoating on Fe₂O₃ and other related electrode materials.

In another recent study, Chidsey and coworkers³⁷ demonstrated that the ALD of an ultrathin conformal oxide could function as protecting layer for silicon photoanodes for water oxidation. The layered structure of a protected Si electrode is shown in Fig. 3(b). Even though the silicon bandgap of 1.1 eV is too small to achieve water splitting, silicon is an interesting photoanode material due to its: (1) large theoretical photocurrent (~ 40 mA/cm²), (2) wide natural abundance,

and (3) well-understood and controlled chemical and physical properties. However, silicon rapidly oxidizes under PEC water oxidation conditions preventing it from performing well in tandem water splitting devices.²¹ Although different methods, including vapor deposition^{29,30} and doping,³⁸ have been adapted for protecting Si photoanodes, they have generally not been successful, possibly due to defects in the protecting layer or increased resistance due to excessive coating thickness blocking hole transport to the semiconductor-electrolyte interface. Chidsey *et al.*³⁷ found that 2 nm of conformal TiO₂ deposited by ALD acts effectively as the protecting layer and simultaneously allows carrier tunneling. It is interesting to point out that Thimsen *et al.* have found that TiO₂ ALD alone (up to 30 nm) could not protect Cu₂O.³⁵ These apparently contradictory results could possibly be due to the different surface nucleation phenomena in ALD deposition on substrates with different surface chemistries, e.g., Si–OH versus Cu–O_x, with different ALD chemistries, (tetraakisdimethylamido titanium versus titanium tetraisopropoxide), under different growth temperatures (200 °C versus 120 °C). This indicates that understanding and controlling the ALD surface deposition mechanism on different substrates is indeed necessary to obtain the designed material properties.

C. Atomic layer deposition for synthesizing photoelectrodes

In addition to protective layers, ALD can also be used to deposit active semiconductor layers for PEC water splitting. Liu *et al.* have utilized ALD to coat TiSi₂ nanonets with TiO₂,³⁹ which serves as the photoactive layer. The as-synthesized TiSi₂/TiO₂ nanostructure, as shown in Fig. 3(c), provides a larger photocurrent than a TiO₂ ALD film alone owing to the high surface area conductive TiSi₂. The ALD process offers several unique advantages here. First, the precise thickness control from ALD of TiO₂ enables optimization of the tradeoff between the light absorption, for which the optimal thickness is close to the depletion layer width, and charge separation, for which a thinner film is better. Secondly, the capability of ALD to coat complex three dimensional (3D) structures with uniform and conformal films offers another degree of engineering capability. It enables increased light absorption due to the higher overall surface area in the nanostructured TiSi₂ relative to the projected area. The same authors used ALD in a more sophisticated way to dope the TiO₂ anatase matrix with W by adjusting WO_x and TiO₂ ALD cycle ratio.³⁹ This lowers the bandgap of TiO₂ and enables visible light absorption as illustrated in Fig. 3(d). In similar fashion, Lin *et al.* synthesized a nanonet of TiSi₂/Fe₂O₃, where Fe₂O₃ was coated onto TiSi₂ with ALD (Ref. 40) and reported 2.7 mA/cm² of photocurrent. The ultrathin Fe₂O₃ coating and the underlying conductive TiSi₂ enhanced charge collection.⁴⁰

ALD was also used by Liu *et al.* to synthesize WO₃,⁴¹ which is a widely studied compound as the water oxidation electrode material with an overall efficiency close to 1%. It should be noted that the WO₃ ALD process in this work

used the precursor [(*t*-BuN)₂(Me₂N₂)W], which does not involve the corrosive byproducts generated by the usual W ALD precursor (WF₆).⁴² This mitigates the environmental concerns associated with fluorinated compounds.

D. Prospects for ALD in photoelectrochemical water splitting devices

Although there are only a few published studies, ALD has been shown to be a very promising method for tuning the interfacial chemical and physical properties of the electrodes in PEC water splitting processes. Although semiconductor based PEC devices are the primary focus of current ALD research. It could potentially find applications in other types of PEC water splitting devices.^{16,17,19} As an advanced atomic-level material engineering technique, ALD has exceptional potential for water splitting and solar fuel research in the following topics in the future.

1. Bandgap engineering for photoelectrochemical electrodes

Bandgap engineering is the process of tuning of the energetics of materials to achieve desired device properties. Few materials studied to date provide a visible-light active photoelectrodes capable of generating electrons and holes with enough energy for water reduction and oxidation, along with chemical stability. There is very little reported research about using ALD to engineer photoelectrode bandgaps and band energies. Owing to the layer-by-layer growth process, ALD can precisely dope or alloy a material and tune its bandgap. For example, Torndahl *et al.* demonstrate that the bandgap of MgO doped ZnO is tunable from 3.2 to 4.0 eV by adjusting the MgO cycle ratio in the ALD process.^{43,44} Then ALD Mg_xZn_{1-x}O film has been successfully used as a buffer layer for improving the CIGS (Cu(In,Ga)Se₂) solar cell efficiency.⁴³ As another example, the ZnO(S) bandgap can be adjusted by tuning the ZnS/ZnO cycle ratio during the ALD. This has been demonstrated by several groups,^{45,46} and has been successfully used as a buffer layer for CIGS based solar cells.⁴⁵ Cd_xZn_(1-x)S is another example of a material that has a tunable bandgap by tuning Cd composition through the ALD process.⁴⁷ In general, other types of doped materials with tuned properties are also possible with ALD, including, e.g., oxides, (oxy)nitrides, (oxy)sulfides, and others. In conjunction with the high conformality of ALD film, precise thickness controllability and large library of ALD chemistries, this strategy will provide a general useful method for engineering electrodes, especially those with complex morphologies and high surface area, to form the protecting layer or heterojunctions for improved light harvesting and incident photon-to-fuel efficiency.

The ALD approach could also potentially contribute towards the optimization of interfacial energetics for photoelectrodes by chemically change the surface condition of the electrodes.^{7,48} It has been shown that surface grafted molecular layers can tune the band edge position of semiconductor photoelectrode.^{49,50} ALD is an excellent process for chemically modifying substrates with sub to monolayers of

different molecules.^{7,9} This, in principle, can provide beneficial applications in grafting designed functional molecules for tuning surface dipole properties, band edges, and surface state density of the electrodes.

2. Catalyst engineering for photoelectrochemical electrodes

Catalyst engineering is another key strategy for achieving more efficient PEC water splitting.^{12,15,51–53} The photo-generated electron or hole can transfer from the host photoelectrode to the corresponding catalyst, which will trap it and kinetically promote the water reduction or oxidation. Noble metals, including Pt, Au, Pd, Ag, and Rh, and metal alloys,^{12,15} have been widely used as catalysts for water reduction to improve reaction rates. RuO₂, NiO, IrO₂, and Co₃O₄^{12,15,19} are common useful catalysts for the water oxidation reaction. Typically, noble metal or metal oxide catalysts are loaded onto photoelectrodes as nanometer-sized colloidal particles. The properties of these catalysts depend on their size, crystal structure, shape, and composition as well as the substrate.⁵⁴

ALD is emerging as a useful method to engineer catalyst particles at the atomic level.^{55–59} As demonstrated by Christensen *et al.*, Pt nanoparticles with tunable diameters of 0.5–2.5 nm are synthesized on high surface area substrates simply by varying the number of ALD cycles. In a similar fashion, Feng *et al.* showed that Pd nanoparticles can also be synthesized by ALD. Furthermore, by taking advantage of the layer-by-layer growth mode in ALD, well-controlled Pt-Ru (Ref. 59) and Ir-Pt (Ref. 58) alloy nanoparticles with tunable size and composition were synthesized by changing the cycle number and the cycle ratio of corresponding ALD processes. Owing to the development of noble metal⁶⁰ and transition metal ALD processes,⁶¹ one can imagine a large number of different catalyst nanoparticles with tunable properties that can be synthesized by ALD. Surface passivation layers, such as organic ligands, which typically result from solvothermal and hydrothermal nanoparticle synthetic methods are avoided with the ALD process. This passivation layer is used to protect the catalyst from sintering and is undesirable for catalysis applications.⁵⁴ More interesting, ALD has been creatively used by several groups^{57,62} to protect the catalyst from sintering in a high temperature reaction environment. This principle could be readily extended to protect catalysts on PEC electrodes to extend catalyst lifetimes. It is also possible to synthesize complex catalyst nanoparticles using ALD, e.g., core-shell, yolk-shell, etc., to achieve desired properties. Although there is few research studies on catalyst engineering by ALD for PEC water splitting application, ALD will have a tremendous opportunity in this field.

3. Nanostructure engineering for photoelectrochemical electrodes

Nanostructured materials have attracted significant interest for improving the performance of photoelectrodes in PEC cells owing to their unique properties, including decoupled light absorption and charge carrier diffusion,^{12,15}

high junction areas between electrolyte and electrodes,^{12,15} and high densities of reactive sites on electrodes.^{12,15} Moreover, the surface area of the nanostructured electrodes has an optimal value for the following reasons: (1) while a large photocurrent can be achieved with a photoelectrode of larger surface area, the photovoltage decreases with increasing junction area (≥ 60 mV per order of magnitude increase in junction area)¹² and (2) light absorption increases with the surface area of the nanostructured electrodes. As a result, the dimensions of the features inside of nanostructured photoelectrodes should be comparable to the charge diffusion length, while simultaneously providing an optimal surface area for achieving higher photovoltage and maximal light absorption. ALD is a powerful technique for synthesizing various kinds of nanostructures including nanotubes, porous nanomaterials, nanospheres, core-shell nanomaterials, and other more complex nanostructured materials.^{9,63,64} With its unique film thickness controllability, ALD offers a unique opportunity to optimize the surface area of nanostructured materials to advance PEC performance.

III. PHOTOELECTROCHEMICAL REGENERATIVE SOLAR ELECTRICAL DEVICES

A. Introduction of photoelectrochemical regenerative solar electrical device

Photovoltaic devices directly convert solar energy to electrical energy, and are currently dominated by Si and other solid state junction devices. Those devices generally suffer from high costs per watt and there is a concern over the future costs due to the low earth-abundance of some of the materials used. There is an increasing awareness that truly scalable photovoltaic devices are only possible if they are fabricated using low-cost processes with earth-abundant materials.^{4,65–67} PEC regenerative cells represent an alternative device design to convert photon energy into electric power. In these devices, the solid state junction is replaced by a semiconductor/electrolyte (polymer, liquid or gel) junction containing a reversible redox couple. Photons with energy larger than the band gap excite electrons, and leave holes in the valence band. Under the electrical field generated by the depletion layer, a photogenerated electron moves through the bulk of the semiconductor to the current collector, then to the counter electrode through an external circuit. At the counter electrode the electrons will reduce the oxidized form (A) of the redox couple to produce an electron donor D.⁴ The positive holes are driven to the semiconductor surface to oxidize the reduced form (D) of the redox couple to the oxidized electron-accepting form, A. In order to achieve high photocurrents, small bandgap semiconductors (< 2 eV) are favorable; however, semiconductors with such a small bandgap are generally not stable under the electrochemical environment.

The dye sensitized solar cells^{65,66,68} (DSSC) is one type of regenerative PEC device that decouples the light absorption and charge-generating functions. The simplified principle of DSSC is shown in Fig. 4.⁴ In these devices, a visible-to-near infrared (NIR) chromophore (also known as dye or sensitizer,

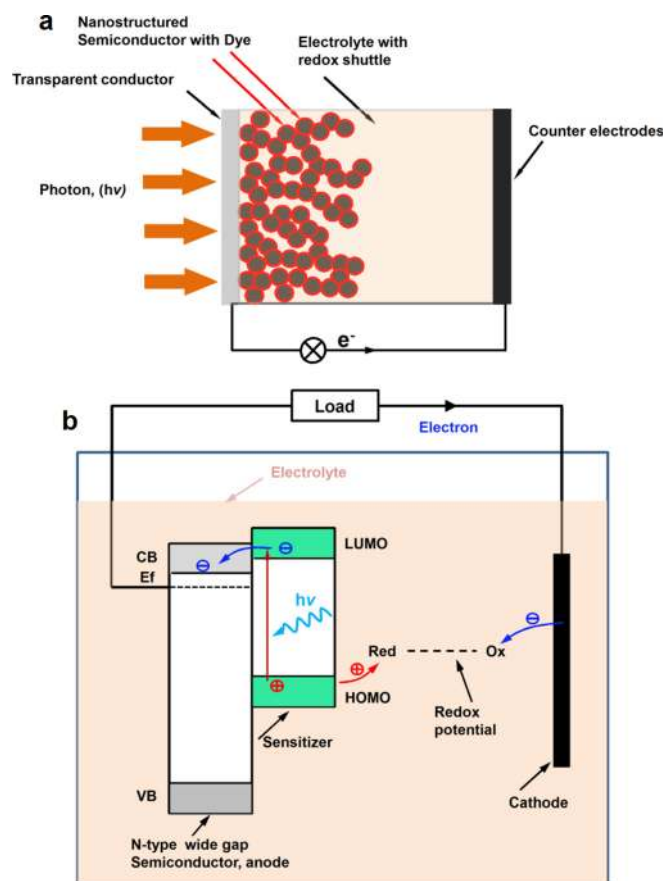


FIG. 4. (Color online) (a) Simplified diagram for Dye sensitized solar cell. Dye molecules adsorbed onto nanostructured semiconductor surface. After excited by photon, dye molecules will inject an electron into conduction band of semiconductors. The oxidized dye molecules will be reduced by the redox shuttle. The oxidized redox species will be reduced on the counter electrode by the electrons from the photoanode through external circuit. (b) Diagram of electron and hole transport inside of the DSSC cell, “Red” and “Ox” are the reduction and oxidation status of redox couple correspondingly. LUMO: lowest unoccupied molecular orbital; HOMO: highest occupied molecular orbital.

e.g., Ru(II) polypyridyl coordination compounds, quantum dots, organic dye) is attached to the surface of a nanostructured wide bandgap semiconductor such as TiO₂. Light absorption by the sensitizer produces an excited state which injects electrons into the acceptor states of the n-type semiconductor. Since 1991,⁶⁵ extensive research in dye engineering and semiconductor nanostructures implementation, including nanoparticles, nanotubes, nanorods, and nanofibers, has optimized the performance of DSSCs. For a single junction DSSC cell, an efficiency of ~11% has been reported.⁶⁶ In order to improve the efficiency further, three components need to be engineered: (1) dye molecule with bandgap that extends photon absorption into the NIR without sacrificing injection yields and oxidized dye regeneration rates, (2) maximizing open circuit voltage by increasing the energy difference between the Fermi level of the semiconductor and the redox couple, and (3) an engineered photoanode that minimizes charge carrier recombination while promoting charge collection. Many review articles on DSSCs already exist.^{66,68–71} Here, we will focus on photoanode engineering by ALD.

B. Surface passivation by ALD to minimize charge recombination

A DSSC photoelectrode needs to satisfy the following requirements to maximize efficiency: (1) highly transparency in the visible to avoid competitive light absorption with the dye, (2) high surface area to enable high loading of surface-attached sensitizers, (3) high carrier collection efficiency, and (4) long carrier diffusion length. Electrons injected from dye molecules into n-type semiconductors, e.g., TiO₂, ZnO, SnO₂, etc., need to be transported to the transparent conducting oxide current collector while avoiding recombination with the oxidized form of the redox shuttle, e.g., tri-iodide and dye. Charge recombination (or back electron transfer reactions) needs to be minimized in order to optimize the energy conversion efficiency of the DSSC. The electron diffusion length (L , $L = \sqrt{D_e \tau_e}$, where D_e is the electron diffusion coefficient and τ_e is the electron lifetime), is a key parameter used to optimize the nanostructured semiconductor film thickness (d), which needs to be smaller than L for quantitative collection of electrons through the film. On the other hand, to maximize light harvesting, d needs to be significantly larger than the light absorption length $1/\alpha$ (where $\alpha = \epsilon c$, where ϵ and c are the molar absorption coefficient and molar concentration of sensitizers, respectively). The unique nature of ALD has been creatively utilized by several groups to address this challenge.

In 2006, Yang *et al.* demonstrated that thin layers of anatase TiO₂ ALD film [as shown in Fig. 5(a)] with thickness between 10 and 35 nm can improve the energy conversion

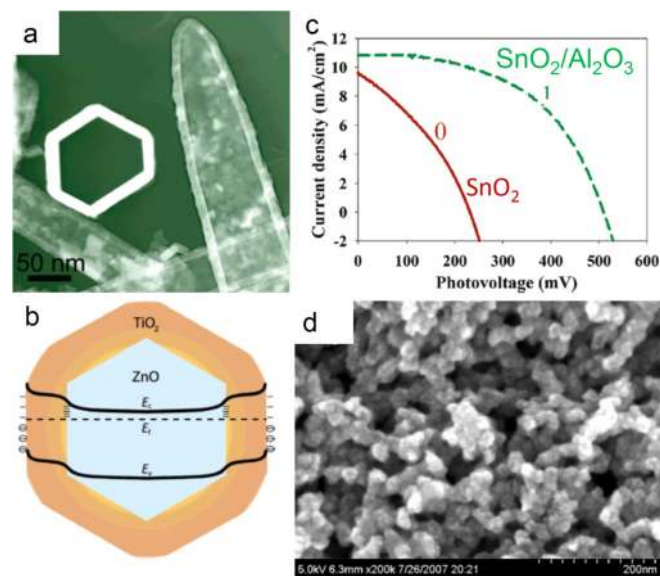


FIG. 5. (Color online) (a) Negative TEM image of anatase nanotubes made by ALD after removing the ZnO wire cores (Ref. 72). (b) Interfacial energetics of ZnO nanowire coated with TiO₂, where electrons flow from TiO₂ to ZnO. Reprinted with permission from Ref. 72 (copyright 2006 American Chemical Society). (c) J-V curves for DSSCs based on naked SnO₂ (solid line) and on SnO₂ coated with one cycle of Al₂O₃ (dashed line). Reprinted with permission from Ref. 74 (copyright 2010 American Chemical Society). (d) Aerogel scaffold coated with 8.4 nm ZnO ALD process. Reprinted with permission from Ref. 75 (copyright 2008 Wiley-VCH).

efficiency of a ZnO nanowire DSSC cell⁷² and hybrid solar cell⁷³ with values up to 2.25% under 100 mW cm⁻² air mass 1.5. The TiO₂ ALD layer⁷² was believed to suppress recombination by surface passivation, and improve charge carrier collection by modifying the band bending between the TiO₂ and ZnO as presented in Fig. 5(b). The authors also found that a thin layer of Al₂O₃ ALD coating improved the open-circuit voltage of the ZnO nanowire DSSC cell, which was also attributed to the suppression of charge recombination. However, a large decrease in short-circuit current density was also observed due to the large energy barrier to charge transport introduced by the Al₂O₃ layer, which reduced the overall energy conversion efficiency. Similarly, decreased current density was observed by Prasittichai *et al.*⁷⁴ when Al₂O₃ was deposited with multiple ALD cycles on the SnO₂ photoanode in a DSSC cell. However, as shown in Fig. 5(c), one cycle of Al₂O₃ ALD passivated the SnO₂ photoelectrode and caused a slightly increased short circuit current density as well as approximately a two-fold increase in the open circuit photovoltage,⁷⁴ corresponding to an increased efficiency from 0.76 to 3.7%. The authors ascribed this improvement to the passivation of surface states that existed in the SnO₂ by submonolayer ALD Al₂O₃ (< 1.5 Å) deposited in a single cycle.⁷⁴ This result demonstrates the unique capability of the ALD for modifying electrode surface from both electronic and chemical aspects, compared with previous methods.⁶⁷

C. Nano-engineered photoelectrodes using ALD

Nanowire based DSSC cells⁷² offer a promising alternative to the traditional colloid-based TiO₂ cell due to high electron mobility and a simpler charge transport path; however, efficiency has been limited by the low surface area enhancement factor of the nanowires (i.e., total surface area/projected surface area < 200 vs > 1000 for colloidal systems). Several strategies have been demonstrated to overcome this limitation. For example, Hamann *et al.* functionalized an inert high specific surface area silica aerogel (> 1000), shown in Fig. 5(d), with ZnO (Ref. 75) and TiO₂ (Ref. 76). ALD for application as the photoanode in DSSC and achieved energy conversion efficiency of ~2.5 and 4.3%, respectively. The efficiency is less than the optimized Gratzel cell with a similar area enhancement factor,⁴ and is attributed to the lower diffusion rate of the redox shuttle within the aerogel matrix.⁷⁶ ALD films have also been deposited onto anodic aluminum oxide (AAO) membranes for solar cell devices. Martinson *et al.* showed that ZnO nanotubes could be grown conformally throughout the porous membrane for application as photoanode of a DSSC.⁷⁷ The surface area enhancement factor of the AAO membrane was ~450, which could be further tuned with the pore size and depth. Furthermore, the multilayered structure of transparent conductor/semiconductor nanotube deposited onto AAO by ALD was shown to have better electron collecting behavior than the semiconductor alone owing to the radial electron collection by the transparent conductor underneath the semiconductor.⁷⁸

D. Prospects for ALD in photoelectrochemical regenerative solar cells

As discussed above, ALD shows great promise to tune the photoanode properties in DSSCs. The most efficient DSSC cells have an absorbed photon-to-current efficiency close to unity, which indicates that there is very limited room to improve the overall efficiency by further optimizing carrier collection properties of the electrode. However, in order to optimize the DSSC to achieve efficiencies exceeding 11%, new dyes and new redox shuttles need to be implemented. Systematic optimization of the photoanode materials for improved dyes and redox shuttles may require new engineering approaches, where ALD could play an important role to, e.g., passivate surface states, introduce desired band energetics for carrier flow, and improve carrier lifetimes.

IV. ATOMIC LAYER DEPOSITION FOR ELECTROCHEMICAL ENERGY CONVERSION

Improving the efficiency of conversion of chemical energy into electrical energy presents a tremendous opportunity for the energy sustainability. Compared with normal turbines, fuel cells potentially offer a much higher energy conversion efficiency, less pollution, and lower green house gas emissions.⁵ Similar to other types of electrochemical systems, electrodes and electrolyte are involved in fuel cells. To optimize fuel cell operating efficiency, new materials development is critical.

Solid oxide fuel cells (SOFCs), whose operating principle is shown schematically in Fig. 6(a), using H₂ as the fuel source, have advantages of relatively flexible fuel composition, less noble metal catalyst required and less fuel crossover, in comparison with other types of fuel cells.⁵ On the other hand, SOFCs suffer from high operating temperatures (500–1000 °C) which are required to achieve sufficient ionic conductivity in the solid oxide electrolytes.^{5,79} A lower

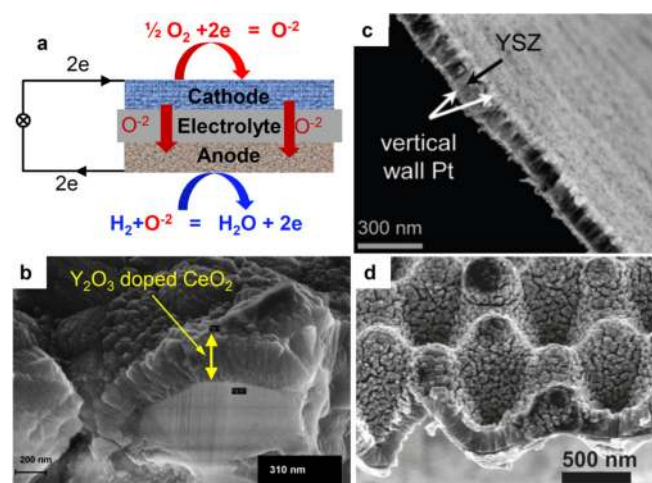


FIG. 6. (Color online) (a) Simplified scheme for solid oxide fuel cell. (b) SEM image of Y₂O₃ doped CeO₂ by ALD. Reprinted with permission from Ref. 87 (copyright 2009 American Chemical Society). (c) SEM image of ALD YSZ thin film (~70 nm) with Pt sputtered on both sides. Reprinted with permission from Ref. 90 (copyright 2008 American Chemical Society). (d) SEM image of nanostructured YSZ electrolytes by sphere lithography. Reprinted with permission from Ref. 91 (copyright 2011 American Chemical Society).

operating temperature would be beneficial for practical applications including mobile electrical supplies, small stand-by power stations, etc.⁷⁹ However, this must be achieved without compromising the electrode kinetics or increasing the series resistance of the cell. In this regard, scaling the fuel cell components down to thin films ($< 1 \mu\text{m}$) provides several advantages:⁷⁹ (1) lower ohmic loss from electrode and electrolytes due to the decreased area specific resistance from the decreased thickness, (2) increased ionic conductivity due to the reduced thickness and increased grain boundary area; and (3) improved reaction kinetics due to the enhanced reactant activation and exchange rates on the nanocrystal grain boundaries.

ALD has been shown as an effective method for helping address these materials related challenges in fuel cells. Casir *et al.* provided a review of ALD work on SOFCs.⁸⁰ ALD has been used to synthesize thin ion conducting solid electrolytes, including yttria-stabilized zirconia (YSZ), a common electrolyte for SOFC.^{81–84} Shim *et al.* showed that the fuel cell fabricated with ALD YSZ electrolyte (60 nm thick) achieves a peak power density of 270 mW/cm^2 at 350°C ,⁸² which is greater than the power density (130 mW/cm^2) of a cell with sputter deposited YSZ electrolyte (50 nm thick) at the same temperatures.⁸⁵ The improved power density is possibly a result of the denser nanograin structure formed during ALD.⁸² Doped CeO_2 electrolyte was also explored by ALD owing to its high ionic conductivity. Gourba *et al.* prepared Gadolinium (Gd) doped CeO_2 by ALD.⁸⁶ Ballée *et al.* showed that it is also possible to deposit Y_2O_3 doped CeO_2 by ALD [Fig. 6(b)] with well-controlled stoichiometry.⁸⁷

Due to the capability of finely tuning the composition of alloy mixtures, ALD can tune electrolytes, such as YSZ, with an ultra thin layer of material with different electrical and ionic properties to enhance fuel cell performance. For instance, Chao *et al.* modified bulk YSZ electrolytes (8 mol. % of yttrium) with an ultrathin ($\sim 1 \text{ nm}$) YSZ film with higher yttrium mole ratio (19 mol. %) by ALD, which led to a 50% increase in power density.⁸⁸ Moreover, Fan *et al.* observed that fuel cell performance was improved by modifying the bulk YSZ electrolytes with a thin Y_2O_3 doped CeO_2 ALD film.⁸⁹ These enhancement effects were ascribed to improved oxygen reduction and exchange properties of the ultrathin ALD layer compared with the underlying electrolytes.^{88,89} This interfacial modification is expected to improve other SOFCs and even other types of fuel cells. The capability of ALD for coating 3 D complex morphology has also been explored for a high surface area thin film SOFC for further efficiency improvements, as shown by the example in Fig. 6(c)⁹⁰ and Fig. 6(d).⁹¹ The large electrochemically active surface area improved the peak power density. Due to the expanding list of materials available by ALD, it is expected that the number of engineered solid electrolytes with tuned properties such as thickness, doping, ionic, and electrical conductivity that are synthesized by ALD will continue to increase.

Compared with the studies of electrolyte development by ALD, limited research has been performed on electrode materials by ALD. Holme *et al.* developed an ALD process for

LSM ($\text{La}_x\text{Sr}_{1-x}\text{MnO}_3$), which is a cathode material for SOFCs.⁹² Another cathode material $\text{La}_x\text{Ca}_{1-x}\text{MnO}_3$ has been synthesized through ALD by Nilsen *et al.*⁹³ In addition to the application of ALD to electrodes and electrolytes in SOFCs, another exciting opportunity for ALD is to synthesize novel catalysts for more efficient SOFCs. Jiang *et al.* used ALD to deposit Pt catalysts and achieved comparable peak power densities with other Pt deposition methods.⁹⁴ A self-assembled monolayer patterned Pt film formed by ALD shows more efficient current collection.⁹⁴ Moreover, the capability of ALD to synthesize catalysts consisting of composites of noble metals^{56,58,59} will benefit this field. More importantly, it would be very interesting to develop new ALD processes for synthesis of catalysts of nonprecious metals^{7,8,10,61} which will have the additional benefits of lowering dependence on expensive noble metals. This potential of ALD would benefit not only the SOFC, but also other types of fuel cells where noble metal catalysts are currently employed.

V. ATOMIC LAYER DEPOSITION FOR ELECTROCHEMICAL ENERGY STORAGE

In addition to the challenges of generation of clean primary energy, a closely related and interdependent issue is energy storage.⁹⁵ High capacitance energy storage with long lifetime is critical for next generation vehicles that do not rely on fossil fuel and is also important for renewable energy due to the temporal and spatial heterogeneity of sunlight, wind, ocean waves, etc.³ Energy storage is also important for next generation mobile computing devices. Among the large family of energy storage technologies, lithium ion batteries represent the most promising technology due to their relatively high energy storage density [$\sim 200 \text{ Wh/kg}$ (Ref. 96)] and acceptable lifetime.^{95,96}

Engineering materials to improve the power capacity and lifetime of the lithium ion battery continues to be a focus for this research field.⁹⁶ Similar to other electrochemical devices, lithium ion batteries also require well-engineered electrodes, electrolytes, and interfaces between the two.⁹⁶ In order to completely solve the challenges, a systematic optimization approach to materials development for all of those components is necessary.⁹⁶ There are already a lot of reviews on this topic.^{95–97} Here we will focus on the application of ALD for addressing the problems faced by the lithium ion battery system.

It has been recognized that the solid-electrolyte interphase (SEI) formed during cycles of the lithiation reaction is one of the main causes of the degradation of electrodes. Side reactions during the cyclic charge/discharge processes also degrade the electrode capacitance. A thin coating onto the electrodes is an effective way to alleviate these effects. Recently an ultrathin coating of Al_2O_3 prepared by ALD shows promise to improve the cycle durability of electrode materials such as LiCoO_2 ,^{98,99} $\text{LiNi}_{1/3}\text{Mn}_{1/3}\text{Co}_{1/3}\text{O}_2$,¹⁰⁰ MoO_3 ,¹⁰¹ graphite,¹⁰² and Si.^{103,104} The effect of an ultrathin Al_2O_3 ALD coating on the durability and conductivity of these electrode materials depends strongly on its thickness. For example, with only two cycles of Al_2O_3 ALD, LiCoO_2

displayed improved capacity retention (89%) compared with bare uncoated electrodes (45%) after 120 charge-discharge cycles under the same experimental conditions.⁹⁸ However, the capacity of LiCoO₂ decreased from ~120 mAh/g to less than 20 mAh/g when the ALD Al₂O₃ cycle increased from 6 to 10, which is ascribed to the dramatic impedance increase caused by the thicker layer.⁹⁸ Similar phenomena were observed for other electrode materials modified by ALD.¹⁰⁰

The complex morphology and large internal surface area of the electrodes makes ALD an excellent method for modifying these materials. As shown in Fig. 7(a), dramatic improvements in durability have been achieved for ALD-coated graphite anodes in comparison to the bare graphite electrode and the electrode consisting of active graphite powder particles coated separately by ALD. This was ascribed to the unaffected interparticle electron conduction pathway and protected active powders surface in electrodes by ALD as illustrated in Fig. 7(b).¹⁰² Nanoscale materials have shown great promise for better durability than corresponding bulk electrode materials for lithium ion batteries electrodes.^{105–107} Recently, ALD was further utilized to coat such as-fabricated composite electrodes consisting of nanoscale materials, such as LiCoO₂ and MoO₃, binder and acetylene black.^{99,101} Figures 7(c) and 7(d) shows the interface between ALD coating and LiCoO₂ and the corresponding

performance of the electrodes with different ALD treatments.⁹⁹ This principle could be adapted into other materials system, such as nanostructures of Si.^{103–107}

These observations highlight the capability of ALD for precision materials engineering in applications of lithium ion batteries.^{98–102,108,109} In the meantime, we are reminded that in order to achieve further improvement, the detailed mechanism for the dramatic thickness dependent performance deserves further study, although some investigations are reported in the literature.^{103,110} In particular, the surface reaction mechanism of ALD onto the electrode materials needs to be investigated since ALD is highly dependent on the surface chemistry and other substrate conditions.^{7,8,10} Furthermore, since two cycles of Al₂O₃ ALD will not cover the surface completely^{10,98,99} if we assume the ideal ALD scheme, it is very possible the Al-O simply passivates some surface defects sites, which are generally more energetic and easier for carrying out chemical reactions; therefore degrading the electrode performance through SEI formation during initial cycles. This surface passivation principle could be potentially adapted into other types of electrochemical energy storage devices, such as supercapacitors, for improving their durability, safety and capacitance. It is worth to note that, owing to its unique coating capability, ALD has recently been adapted for synthesis of active components for three dimensional all-solid-state

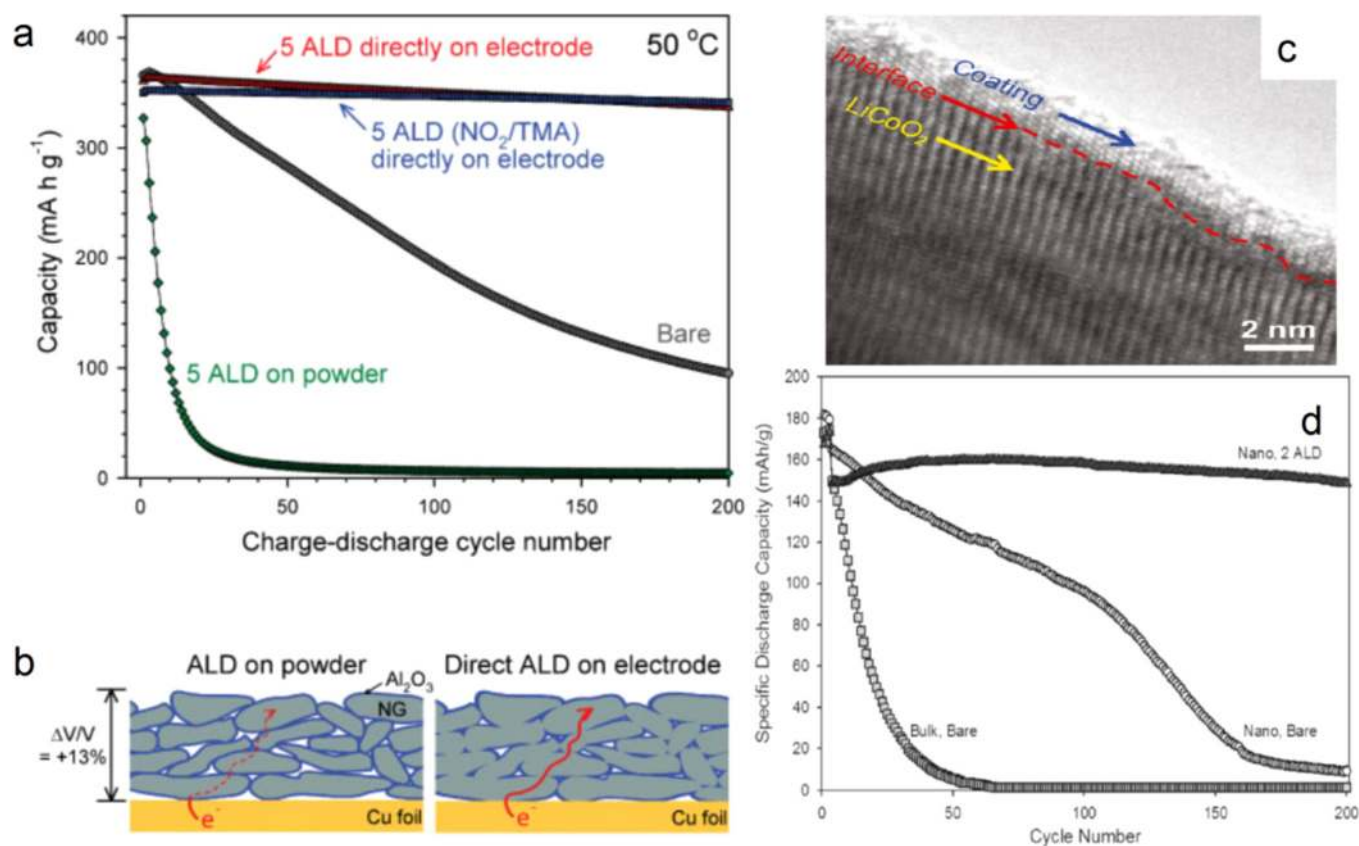


FIG. 7. (Color online) (a) Comparison of the electrochemical performance of electrodes consisting of bare natural graphite (NG), ALD coated NG powder, and NG composited electrodes coated directly by ALD with different chemistries (Ref. 102). (b) The schematic diagram of electron transport in NG composite electrodes prepared by ALD on powder and ALD directly on the electrode. Reprinted with permission from Ref. 102 (copyright 2010 Wiley-VCH). (c) TEM image of Al₂O₃ ALD coated LiCoO₂ particles (Ref. 99). (d) Comparison of performance electrodes consisting of bulk LiCoO₂ particle, LiCoO₂ nanoparticles before and after ALD treatment. Reprinted with permission from Ref. 99 (copyright 2011 American Chemical Society).

lithium-ion microbattery.¹¹¹ Although only a few works have been done to date,^{111–113} ALD will play an important role in the field in the near future.

VI. OUTLOOK

The preceding discussion shows ALD as a promising technique for electrochemical-based energy generation, conversion and storage. In order for ALD to achieve greater impact in both the scientific and practical energy research, some important issues must be addressed. We present next some key issues that in our opinion could be readily addressed.

A. *In situ* and *in vacuo* investigation of ALD process on electrochemically important substrates

As has been discussed,^{7–10} the substrate surface conditions, including reaction site type and density, crystal structure, and substrate chemistry, have dramatic effects on the materials growth behavior in ALD.^{7–10} Moreover, ALD process parameters, including reaction temperature, pressure, and precursor and coreactant chemistry, also dramatically influence the film quality, crystallinity and interfacial properties.^{7–10} Therefore, in order to achieve good control of the deposited film and the interface between an ALD coating and the underlying substrate, it is necessary to directly probe the surface reactions. Various *in situ* and *in vacuo* techniques provide the optimal means to explore these reactions. Techniques of interest include synchrotron x ray analysis,^{114,115} x ray photoelectron measurements,¹¹⁶ quartz crystal microbalance analysis,¹¹⁷ Fourier transform infrared spectroscopy,¹¹⁸ scanning probe microscopy,¹¹⁹ ellipsometry, and transmission electron microscopy¹²⁰ as well as electrical properties analysis.¹²¹ These measurements will provide complementary information about the surface reactions and molecular processes of the ALD on the substrates, which in turn will help identify the right ALD process conditions for the desired materials and interfacial properties.

B. Exploring new ALD processes

One of the biggest advantages of ALD over other thin film deposition methods is its capability to coat high surface area substrates with complex morphologies and high aspect ratio features, which are commonly observed in electrochemical system, with an ultrathin, conformal and uniform materials.^{7–10} For such purposes, thermal ALD is preferred, because thermal energy can be delivered into substrates with high specific surface area much more uniformly than other energy sources, e.g., plasma and photon. In order to maintain the surface limited growth behavior and eliminate the less controllable thermal decomposition of reactants, the growth temperature of ALD is generally kept low enough (< 350 °C) to prevent the precursor from decomposing.⁷ The low deposition temperature can lead to inferior material quality, such as crystal structure, defects, low density and nonstoichiometric composition. Although plasma-based ALD has been adapted for improving material quality, the less conformal step coverage from plasma processes presents a challenge due to the lifetime of radicals.

Since the properties of ALD materials strongly depend on the chemistries used in the deposition,^{7–10,122} new thermal ALD processes capable of better material quality need more attention. With past and current ALD development, most of the chemistries have been directly adapted from metal-organic chemical vapor deposition (MOCVD) processes.¹⁰ Although ALD is closely related to MOCVD, there are dramatically different requirements for the precursors in each case.¹²² For example, for ALD, metal-organic precursors need to have decomposition temperatures higher than the film growth temperatures, whereas in MOCVD growth temperatures often exceed the precursor decomposition temperature.^{7–10,122} Moreover, precursors for ALD need to have specific reaction with surface reaction sites, and as-generated surface sites must be reactive for subsequent surface reactions. This stipulation is not required for MOCVD processes. We expect that significant progress could be made if more specific research is devoted to developing ALD based metal-organic precursors.

With more than 40 years of development, ALD processes of a variety of different metals, metal oxides, metal nitrides, metal sulfides and other complex materials have been developed.^{7,8,10} However, there are still some materials that are difficult to deposit by ALD, including electrochemically important materials such as Ag, Au, Cu, MnO₂, IrO₂, etc. This also requires the development of new ALD chemistries to enable its full usage in electrochemical applications.

An exciting development in ALD is to extend the layer-by-layer heterogeneous molecular assembly reaction mode into synthesizing highly conformal ultrathin films of different classes of materials including organic,^{123,124} organic-inorganic hybrid,^{124–130} and porous coatings.^{125,129} This development would open up great yet-to-explored opportunities to organize organic and/or inorganic components in a vector mode for desired electron and charge transfer properties,²³ chemical properties,¹²³ and structural properties.^{125,129} Owing to the low deposition temperature of many ALD processes, it has also been demonstrated that ALD could be applied to organic substrates such as polymers^{131–133} and biomaterials,¹³⁴ which provides another degree of flexibility for engineering materials of interest in electrochemical applications.

C. Cost reduction and economic evaluation of ALD processes for particular applications

As a highly sophisticated deposition process, ALD is generally considered a time consuming and high-cost process. The cost of the ALD process is primarily a result of the following: (1) the upfront equipment cost, (2) throughput, (3) maintenance of reactor, (4) precursor consumption, and (5) labor. The analysis of economic cost and sustainability of the ALD process is still a relatively unexplored area. For most ALD processes, (1)–(3) are the major components of the cost, especially, the throughput, which depends strongly on the reactor design. Typically, at 100–200 °C deposition temperature, Al₂O₃ ALD process with trimethylaluminum/H₂O can grow materials at a rate of ~1.2 Å/cycle and a cycle time of 2–5 s/cycle. The cycle time could be even longer for

substrates with a high surface area.⁶⁴ It may take hours, even days, to grow hundreds of nanometer or micrometer thick films. Although operation of many ALD systems in parallel could alleviate this problem, it is obvious that for such thick films, ALD is not a very attractive option from an economic perspective. Moreover, in order to push the reaction to finish in a short time and achieve good step coverage, an excessive amount of precursor is generally used in the deposition process ($\sim 10^3$ – 10^6 Torr/cycle), which means that the usage of precursor could be very low ($< 0.1\%$) in ALD processes. Therefore, cost reduction for ALD processes is an essential topic that must be addressed for practical applications given that cost reduction is vital for the success of all the electrochemical energy related processes discussed above. Recently, we note that there is significant effort focused on new high throughput ALD processing techniques, including ALD at atmospheric pressure and in roll-to-roll processes that could eventually enable ALD to be achieved at high overall rate at very low cost.¹³⁵

VII. SUMMARY

This article addresses the current state of knowledge for the application of atomic layer deposition in electrochemical systems, including PEC water splitting, PEC solar cell, electrocatalysis, fuel cells and batteries. Novel applications of new and unique capabilities of atomic layer deposition process for these systems are just now beginning to emerge. It is possible that ALD and related chemical synthesis approaches may provide a key technological advance that will help these environmentally sound energy generation and storage systems become more practical and more efficient, to improve the lives of future generations.

ACKNOWLEDGMENTS

The coauthors gratefully acknowledge funding from RTI International and the Research Triangle Solar Fuels Institute (RTSFI). RTSFI is a consortium consisting of RTI International, Duke University, NC State University, and University of North Carolina at Chapel Hill.

¹N. S. Lewis and D. G. Nocera, *Proc. Natl. Acad. Sci. U.S.A.* **103**, 15729 (2006).

²K. S. Kang, Y. S. Meng, J. Breger, C. P. Grey, and G. Ceder, *Science* **311**, 977 (2006).

³Department of Energy, http://www1.eere.energy.gov/vehiclesandfuels/technologies/energy_storage/, 2011.

⁴M. Gratzel, *Nature* **414**, 338 (2001).

⁵B. C. H. Steele and A. Heinzl, *Nature* **414**, 345 (2001).

⁶A. J. Bard and L. R. Faulkner, *Electrochemical Methods Fundamentals and Applications*, 2nd ed. (Wiley, New York, 2001).

⁷S. M. George, *Chem. Rev.* **110**, 111 (2010).

⁸M. Leskela and M. Ritala, *Angew. Chem. Int. Ed.* **42**, 5548 (2003).

⁹M. Knez, K. Niesch, and L. Niinisto, *Adv. Mater.* **19**, 3425 (2007).

¹⁰R. L. Puurunen, *J. Appl. Phys.* **97**, 121301 (2005).

¹¹A. J. Bard and M. A. Fox, *Acc. Chem. Res.* **28**, 141 (1995).

¹²N. S. Lewis, M. G. Walter, E. L. Warren, J. R. McKone, S. W. Boettcher, Q. X. Mi, and E. A. Santori, *Chem. Rev.* **110**, 6446 (2010).

¹³A. Fujishima and K. Honda, *Nature* **238**, 37 (1972).

¹⁴M. S. Wrighton, *Acc. Chem. Res.* **12**, 303 (1979).

¹⁵X. B. Chen, S. H. Shen, L. J. Guo, and S. S. Mao, *Chem. Rev.* **110**, 6503 (2010).

¹⁶J. H. Alstrum-Acevedo, M. K. Brennaman, and T. J. Meyer, *Inorg. Chem.* **44**, 6802 (2005).

¹⁷T. J. Meyer, *Acc. Chem. Res.* **22**, 163 (1989).

¹⁸M. Gratzel, *Energy Resources Through Photochemistry and Catalysis* (Academic Press, New York, 1983).

¹⁹W. J. Youngblood, S. H. A. Lee, K. Maeda, and T. E. Mallouk, *Acc. Chem. Res.* **42**, 1966 (2009).

²⁰F. Liu, J. J. Concepcion, J. W. Jurss, T. Cardolaccia, J. L. Templeton, and T. J. Meyer, *Inorg. Chem.* **47**, 1727 (2008).

²¹M. Matsumura and S. R. Morrison, *J. Electroanal. Chem.* **147**, 157 (1983).

²²Y. J. Lin, G. B. Yuan, R. Liu, S. Zhou, S. W. Sheehan, and D. W. Wang, *Chem. Phys. Lett.* **507**, 209 (2011).

²³P. G. Hoertz and T. E. Mallouk, *Inorg. Chem.* **44**, 6828 (2005).

²⁴E. Aharonshalom and A. Heller, *J. Electrochem. Soc.* **129**, 2865 (1982).

²⁵O. Khaselev and J. A. Turner, *Science* **280**, 425 (1998).

²⁶S. Licht, B. Wang, S. Mukerji, T. Soga, M. Umeno, and H. Tributsch, *J. Phys. Chem. B* **104**, 8920 (2000).

²⁷R. C. Kainthla, B. Zelenay, and J. O. Bockris, *J. Electrochem. Soc.* **134**, 841 (1987).

²⁸J. Brillet, M. Cornuz, F. Le Formal, J. H. Yum, M. Gratzel, and K. Sivula, *J. Mater. Res.* **25**, 17 (2010).

²⁹P. A. Kohl, S. N. Frank, and A. J. Bard, *J. Electrochem. Soc.* **124**, 225 (1977).

³⁰F. R. F. Fan, G. A. Hope, and A. J. Bard, *J. Electrochem. Soc.* **129**, 1647 (1982).

³¹H. Gerischer, *J. Vac. Sci. Technol.* **15**, 1422 (1978).

³²A. B. Ellis, S. W. Kaiser, and M. S. Wrighton, *J. Am. Chem. Soc.* **98**, 1635 (1976).

³³R. N. Dominey, N. S. Lewis, J. A. Bruce, D. C. Bookbinder, and M. S. Wrighton, *J. Am. Chem. Soc.* **104**, 467 (1982).

³⁴T. Stempel, M. Aggour, K. Skorupska, A. Munoz, and H. J. Lewerenz, *Electrochem. Commun.* **10**, 1184 (2008).

³⁵A. Paracchino, V. Laporte, K. Sivula, M. Gratzel, and E. Thimsen, *Nat. Mater.* **10**, 456 (2011).

³⁶F. L. F. Le Formal, N. Tetreault, M. Cornuz, T. Moehl, M. Gratzel, and K. Sivula, *Chem. Sci.* **2**, 737 (2011).

³⁷Y. W. Chen, J. D. Prange, S. Duhnen, Y. Park, M. Gunji, C. E. D. Chidsey, and P. C. McIntyre, *Nat. Mater.* **10**, 539 (2011).

³⁸A. Q. Contractor and J. O. M. Bockris, *Electrochim. Acta* **29**, 1427 (1984).

³⁹Y. J. Lin, S. Zhou, X. H. Liu, S. Sheehan, and D. W. Wang, *J. Am. Chem. Soc.* **131**, 2772 (2009).

⁴⁰Y. J. Lin, S. Zhou, S. W. Sheehan, and D. W. Wang, *J. Am. Chem. Soc.* **133**, 2398 (2011).

⁴¹R. Liu, Y. J. Lin, L. Y. Chou, S. W. Sheehan, W. S. He, F. Zhang, H. J. M. Hou, and D. W. Wang, *Angew. Chem. Int. Ed.* **50**, 499 (2011).

⁴²J. W. Klaus, S. J. Ferro, and S. M. George, *Thin Solid Films* **360**, 145 (2000).

⁴³T. Torndahl, C. Platzer-Bjorkman, J. Kessler, and M. Edoff, *Prog. Photovoltaics* **15**, 225 (2007).

⁴⁴T. Torndahl, E. Coronel, A. Hultqvist, C. Platzer-Bjorkman, K. Leifer, and M. Edoff, *Prog. Photovoltaics* **17**, 115 (2009).

⁴⁵B. W. Sanders and A. Kitai, *Chem. Mater.* **4**, 1005 (1992).

⁴⁶C. Platzer-Bjorkman, T. Torndahl, D. Abou-Ras, J. Malmstrom, J. Kessler, and L. Stolt, *J. Appl. Phys.* **100**, 044506 (2006).

⁴⁷J. R. Bakke, J. T. Tanskanen, H. J. Jung, R. Sinclair, and S. F. Bent, *J. Mater. Chem.* **21**, 743 (2011).

⁴⁸Q. Peng, B. Gong, and G. N. Parsons, *Nanotechnology* **22**, 155601 (2011).

⁴⁹T. W. Hamann and N. S. Lewis, *J. Phys. Chem. B* **110**, 22291 (2006).

⁵⁰C. M. Wang and T. E. Mallouk, *J. Phys. Chem.* **94**, 4276 (1990).

⁵¹A. B. Bocarsly, D. C. Bookbinder, R. N. Dominey, N. S. Lewis, and M. S. Wrighton, *J. Am. Chem. Soc.* **102**, 3683 (1980).

⁵²S. Trasatti, *J. Electroanal. Chem.* **39**, 163 (1972).

⁵³S. Trasatti, *J. Electroanal. Chem.* **111**, 125 (1980).

⁵⁴G. A. Somorjai, H. Frei, and J. Y. Park, *J. Am. Chem. Soc.* **131**, 16589 (2009).

⁵⁵M. Lindblad, L. P. Lindfors, and T. Suntola, *Catal. Lett.* **27**, 323 (1994).

⁵⁶D. J. Comstock, S. T. Christensen, J. W. Elam, M. J. Pellin, and M. C. Hersam, *Adv. Funct. Mater.* **20**, 3099 (2010).

⁵⁷H. Feng, J. L. Lu, P. C. Stair, and J. W. Elam, *Catal. Lett.* **141**, 512 (2011).

⁵⁸S. T. Christensen and J. W. Elam, *Chem. Mater.* **22**, 2517 (2010).

⁵⁹S. T. Christensen, H. Feng, J. L. Libera, N. Guo, J. T. Miller, P. C. Stair, and J. W. Elam, *Nano Lett.* **10**, 3047 (2010).

- ⁶⁰T. Aaltonen, M. Ritala, Y. L. Tung, Y. Chi, K. Arstila, K. Meinander, and M. Leskela, *J. Mater. Res.* **19**, 3353 (2004).
- ⁶¹B. S. Lim, A. Rahtu, and R. G. Gordon, *Nat. Mater.* **2**, 749 (2003).
- ⁶²J. L. Lu and P. C. Stair, *Angew. Chem. Int. Ed.* **49**, 2547 (2010).
- ⁶³C. Bae, H. Yoo, S. Kim, K. Lee, J. Kim, M. A. Sung, and H. Shin, *Chem. Mater.* **20**, 756 (2008).
- ⁶⁴J. W. Elam, D. Routkevitch, P. P. Mardilovich, and S. M. George, *Chem. Mater.* **15**, 3507 (2003).
- ⁶⁵B. Oregan and M. Gratzel, *Nature* **353**, 737 (1991).
- ⁶⁶M. Gratzel, *Inorg. Chem.* **44**, 6841 (2005).
- ⁶⁷A. Kay and M. Gratzel, *Chem. Mater.* **14**, 2930 (2002).
- ⁶⁸M. Gratzel, *Acc. Chem. Res.* **42**, 1788 (2009).
- ⁶⁹A. Hagfeldt, G. Boschloo, L. C. Sun, L. Kloo, and H. Pettersson, *Chem. Rev.* **110**, 6595 (2010).
- ⁷⁰Z. J. Ning, Y. Fu, and H. Tian, *Energy Environ. Sci.* **3**, 1170 (2010).
- ⁷¹T. W. Hamann, R. A. Jensen, A. B. F. Martinson, H. Van Ryswyk, and J. T. Hupp, *Energy Environ. Sci.* **1**, 66 (2008).
- ⁷²M. Law, L. E. Greene, A. Radenovic, T. Kuykendall, J. Liphardt, and P. D. Yang, *J. Phys. Chem. B* **110**, 22652 (2006).
- ⁷³L. E. Greene, M. Law, B. D. Yuhus, and P. D. Yang, *J. Phys. Chem. C* **111**, 18451 (2007).
- ⁷⁴C. Prasittichai and J. T. Hupp, *J. Phys. Chem. Lett.* **1**, 1611 (2010).
- ⁷⁵T. W. Hamann, A. B. F. Martinson, J. W. Elam, M. J. Pellin, and J. T. Hupp, *Adv. Mater.* **20**, 1560 (2008).
- ⁷⁶T. W. Hamann, A. B. F. Martinson, J. W. Elam, M. J. Pellin, and J. T. Hupp, *J. Phys. Chem. C* **112**, 10303 (2008).
- ⁷⁷A. B. F. Martinson, J. W. Elam, J. T. Hupp, and M. J. Pellin, *Nano Lett.* **7**, 2183 (2007).
- ⁷⁸A. B. F. Martinson, J. W. Elam, J. Liu, M. J. Pellin, T. J. Marks, and J. T. Hupp, *Nano Lett.* **8**, 2862 (2008).
- ⁷⁹D. Beckel, A. Bieberle-Hutter, A. Harvey, A. Infortuna, U. P. Muecke, M. Prestat, J. L. M. Rupp, and L. J. Gauckler, *J. Power Sources* **173**, 325 (2007).
- ⁸⁰M. Cassir, A. Ringuede, and L. Niinisto, *J. Mater. Chem.* **20**, 8987 (2010).
- ⁸¹M. Putkonen, T. Sajavaara, J. Niinisto, L. S. Johansson, and L. Niinisto, *J. Mater. Chem.* **12**, 442 (2002).
- ⁸²J. H. Shim, C. C. Chao, H. Huang, and F. B. Prinz, *Chem. Mater.* **19**, 3850 (2007).
- ⁸³C. N. Ginestra, R. Sreenivasan, A. Karthikeyan, S. Ramanathan, and P. C. McIntyre, *Electrochem. Solid State Lett.* **10**, B161 (2007).
- ⁸⁴C. Bernay, A. Ringuede, P. Colomban, D. Lincot, and M. Cassir, *J. Phys. Chem. Solids* **64**, 1761 (2003).
- ⁸⁵H. Huang, M. Nakamura, P. C. Su, R. Fasching, Y. Saito, and F. B. Prinz, *J. Electrochem. Soc.* **154**, B20 (2007).
- ⁸⁶E. Gourba, A. Ringuede, M. Cassir, J. Paivasaari, J. Niinisto, M. Putkonen, and L. Niinisto, *Microstructural and Electrical Properties of Gadolinium Doped Ceria Thin Films Prepared by Atomic Layer Deposition (ALD)* (Electrochemical Society, Pennington, 2003).
- ⁸⁷E. Balle, A. Ringuede, M. Cassir, M. Putkonen, and L. Niinisto, *Chem. Mater.* **21**, 4614 (2009).
- ⁸⁸C. C. Chao, Y. B. Kim, and F. B. Prinz, *Nano Lett.* **9**, 3626 (2009).
- ⁸⁹Z. Fan, C. C. Chao, F. Hossein-Babaei, and F. B. Prinz, *J. Mater. Chem.* **21**, 10903 (2011).
- ⁹⁰P. C. Su, C. C. Chao, J. H. Shim, R. Fasching, and F. B. Prinz, *Nano Lett.* **8**, 2289 (2008).
- ⁹¹C. C. Chao, C. M. Hsu, Y. Cui, and F. B. Prinz, *ACS Nano* **5**, 5692 (2011).
- ⁹²T. P. Holme, C. Lee, and F. B. Prinz, *Solid State Ionics* **179**, 1540 (2008).
- ⁹³O. Nilsen, E. Rauwel, H. Fjellvag, and A. Kjekshus, *J. Mater. Chem.* **17**, 1466 (2007).
- ⁹⁴X. R. Jiang, H. Huang, F. B. Prinz, and S. F. Bent, *Chem. Mater.* **20**, 3897 (2008).
- ⁹⁵A. S. Arico, P. Bruce, B. Scrosati, J. M. Tarascon, and W. Van Schalkwijk, *Nat. Mater.* **4**, 366 (2005).
- ⁹⁶J. M. Tarascon and M. Armand, *Nature* **414**, 359 (2001).
- ⁹⁷D. R. Rolison, R. W. Long, J. C. Lytle, A. E. Fischer, C. P. Rhodes, T. M. McEvoy, M. E. Bourga, and A. M. Lubers, *Chem. Soc. Rev.* **38**, 226 (2009).
- ⁹⁸Y. S. Jung, A. S. Cavanagh, A. C. Dillon, M. D. Groner, S. M. George, and S. H. Lee, *J. Electrochem. Soc.* **157**, A75 (2010).
- ⁹⁹I. D. Scott, Y. S. Jung, A. S. Cavanagh, Y. F. An, A. C. Dillon, S. M. George, and S. H. Lee, *Nano Lett.* **11**, 414 (2011).
- ¹⁰⁰L. A. Riley, S. Van Ana, A. S. Cavanagh, Y. F. Yan, S. M. George, P. Liu, A. C. Dillon, and S. H. Lee, *J. Power Sources* **196**, 3317 (2011).
- ¹⁰¹L. A. Riley, A. S. Cavanagh, S. M. George, Y. S. Jung, Y. F. Yan, S. H. Lee, and A. C. Dillon, *ChemPhysChem* **11**, 2124 (2010).
- ¹⁰²Y. S. Jung, A. S. Cavanagh, L. A. Riley, S. H. Kang, A. C. Dillon, M. D. Groner, S. M. George, and S. H. Lee, *Adv. Mater.* **22**, 2172 (2010).
- ¹⁰³X. Xiao, P. Lu, and D. Ahn, *Adv. Mater.* **23**, 3911 (2011).
- ¹⁰⁴Y. He, X. Yu, Y. Wang, H. Li, and X. Huang, *Adv. Mater.* **23**, 4938 (2011).
- ¹⁰⁵P. Poizat, S. Laruelle, S. Grugeon, L. Dupont, and J. M. Tarascon, *Nature* **407**, 496 (2000).
- ¹⁰⁶C. K. Chan, H. L. Peng, G. Liu, K. McIlwrath, X. F. Zhang, R. A. Huggins, and Y. Cui, *Nat. Nanotechnol.* **3**, 31 (2008).
- ¹⁰⁷P. G. Bruce, B. Scrosati, and J. M. Tarascon, *Angew. Chem. Int. Ed.* **47**, 2930 (2008).
- ¹⁰⁸S. H. Lee, Y. H. Kim, R. Deshpande, P. A. Parilla, E. Whitney, D. T. Gilaspie, K. M. Jones, A. H. Mahan, S. B. Zhang, and A. C. Dillon, *Adv. Mater.* **20**, 3627 (2008).
- ¹⁰⁹Z. H. Chen, Y. Qin, K. Amine, and Y. K. Sun, *J. Mater. Chem.* **20**, 7606 (2010).
- ¹¹⁰Y. Liu, N. S. Hudak, D. L. Huber, S. J. Limmer, J. P. Sullivan, and J. Y. Huang, *Nano Lett.* **11**, 4188 (2011).
- ¹¹¹J. F. M. Oudenhoven, L. Baggetto, and P. H. L. Notten, *Adv. Energy Mater.* **1**, 10 (2011).
- ¹¹²H. C. M. Knoop, L. Baggetto, E. Langereis, M. C. M. van de Sanden, J. H. Klootwijk, F. Roozeboom, R. A. H. Niessen, P. H. L. Notten, and W. M. M. Kessels, *J. Electrochem. Soc.* **155**, G287 (2008).
- ¹¹³L. Baggetto, H. C. M. Knoop, R. A. H. Niessen, W. M. M. Kessels, and P. H. L. Notten, *J. Mater. Chem.* **20**, 3703 (2010).
- ¹¹⁴K. Devloo-Casier, J. Dendooven, K. F. Ludwig, G. Lekens, J. D'Haen, and C. Detavernier, *Appl. Phys. Lett.* **98**, 231905 (2011).
- ¹¹⁵D. D. Fong, J. A. Eastman, S. K. Kim, T. T. Fister, M. J. Highland, P. M. Baldo, and P. H. Fuoss, *Appl. Phys. Lett.* **97**, 191904 (2010).
- ¹¹⁶A. S. Killampalli, P. F. Ma, and J. R. Engstrom, *J. Am. Chem. Soc.* **127**, 6300 (2005).
- ¹¹⁷J. W. Elam, M. D. Groner, and S. M. George, *Rev. Sci. Instrum.* **73**, 2981 (2002).
- ¹¹⁸J. Kwon, M. Dai, M. D. Halls, E. Langereis, Y. J. Chabal, and R. G. Gordon, *J. Phys. Chem. C* **113**, 654 (2009).
- ¹¹⁹J. B. Clemens, E. A. Chagarov, M. Holland, R. Droopad, J. Shen, and A. C. Kummel, *J. Chem. Phys.* **133**, 154704 (2010).
- ¹²⁰K. H. Min, R. Sinclair, I. S. Park, S. T. Kim, and U. I. Chung, *Philos. Mag.* **85**, 2049 (2005).
- ¹²¹J. S. Na, Q. Peng, G. Scarel, and G. N. Parsons, *Chem. Mater.* **21**, 5585 (2009).
- ¹²²M. Leskela and M. Ritala, *Thin Solid Films* **409**, 138 (2002).
- ¹²³P. W. Loscutt, H. Zhou, S. B. Clendenning, and S. F. Bent, *ACS Nano* **4**, 331 (2010).
- ¹²⁴S. M. George, B. Yoon, and A. A. Dameron, *Acc. Chem. Res.* **42**, 498 (2009).
- ¹²⁵B. Yoon, D. Seghete, A. S. Cavanagh, and S. M. George, *Chem. Mater.* **21**, 5365 (2009).
- ¹²⁶A. A. Dameron, D. Seghete, B. B. Burton, S. D. Davidson, A. S. Cavanagh, J. A. Bertrand, and S. A. George, *Chem. Mater.* **20**, 3315 (2008).
- ¹²⁷B. H. Lee, M. K. Ryu, S. Y. Choi, K. H. Lee, S. Im, and M. M. Sung, *J. Am. Chem. Soc.* **129**, 16034 (2007).
- ¹²⁸B. Yoon, J. L. O'Patches, D. Seghete, A. S. Cavanagh, and S. M. George, *Chem. Vapor Deposition* **15**, 112 (2009).
- ¹²⁹B. Gong, Q. Peng, and G. N. Parsons, *J. Phys. Chem. B* **115**, 5930 (2011).
- ¹³⁰Q. Peng, B. Gong, R. M. VanGundy, and G. N. Parsons, *Chem. Mater.* **21**, 820 (2009).
- ¹³¹C. A. Wilson, R. K. Grubbs, and S. M. George, *Chem. Mater.* **17**, 5625 (2005).
- ¹³²Q. Peng, X. Y. Sun, J. C. Spagnola, G. K. Hyde, R. J. Spontak, and G. N. Parsons, *Nano Lett.* **7**, 719 (2007).
- ¹³³J. S. King, E. Graugnard, O. M. Roche, D. N. Sharp, J. Scrimgeour, R. G. Denning, A. J. Turberfield, and C. J. Summers, *Adv. Mater.* **18**, 1561 (2006).
- ¹³⁴M. Knez, A. Kadri, C. Wege, U. Gosele, H. Jeske, and K. Nielsch, *Nano Lett.* **6**, 1172 (2006).
- ¹³⁵P. Poodt, D. C. Cameron, E. Dickey, S. M. George, V. Kuznetsov, G. N. Parsons, F. Roozeboom, G. Sundaram, and A. Vermeer, *J. Vac. Sci. Technol. A* **30**, 010802 (2011).
- ¹³⁶O. Khaselev, A. Bansal, and J. A. Turner, *Int. J. Hydrogen Energy* **26**, 127 (2001).